BCGS Admissions Academy

Mapping Study of 71 *Planck* Cold Clumps in Taurus/Perseus/California Complexes

Fanyi Meng

Supervisor: Prof. Yuefang Wu

PEKING UNIVERSITY

March 24, 2013

Good afternoon everyone, I am Fanyi Meng from Peking University, PR China. I am a candidate of BCGS Honors Branch. My presentation is about one of our studies: the Mapping study of 71 Planck Cold Clumps in Taurus, Perseus and California Complexes.

My supervisor is Professor Yuefang Wu, from Peking University, Department of Astronomy.

Outline

- Introduction
- Observation
- Results and Analysis
  - Gas Emission
  - Physical Parameters
  - Gas-Dust Coupling
  - Stability of Cores
  - Associated Objects
- Summary

This is the outline of my talk.

1 Introduction

- *Planck* space telescope, working at mm/sub-mm bands, systematically investigated galactic cold dust cores and presented *Planck* Early Release Cold Cores Catalog (ECC).
- ECC contains 915 most reliable (SNR > 15 and $T_{\rm ECC} < 14$ K) detections (Planck Collaboration 2011).
- Besides the dust observation made by Planck Collaboration, study of gas components of these cores is of urgent necessity.
- Millimeter line follow-up studies of Planck Cold Cores were conducted by our group (*ApJ*, 756, 76):
  - A single point survey toward 674 *Planck* Cold Clumps of ECC in the $J = 1 - 0$ transitions of ^{12}CO , ^{13}CO , and C^{18}O has been carried out using the Purple Mountain Observatory 13.7 m Telescope.

As we know, previous sample selection of studying star formation is always on the band of optical or infrared, which led us to know the cores that contain sources or forming stars well. However, Planck telescope, which works at mm/submm band, offer us the opportunities to investigate the pre-stellar cores, which are cold and immature. By analyzing the physical condition of these pre-stellar cores, we can get to know the very early stages of star formation, even the formation of molecular itself, from atomic clouds.

We used the catalog of ECC as our guide, which is the nine hundred and fifteen Planck Cold Clumps with temperature lower than fourteen Kelvin and with SNR exceeding fifteen.

Although that Planck Collaboration has already made the survey of dust component of Planck Cold Cores, study of gas component is still of urgent necessity, because from it we can get to know the dynamic features, chemical composition, equilibrium etc features of these cold cores. Thus, I firstly joined our project of single point millimeter line survey towards six hundred-and-seventy-four Planck Cold Clumps of ECC. We used the J equals to one to zero lines of these three commonly used isotopes of CO and the observation was done using the thirteen-point-seven-meter telescope of PMO.

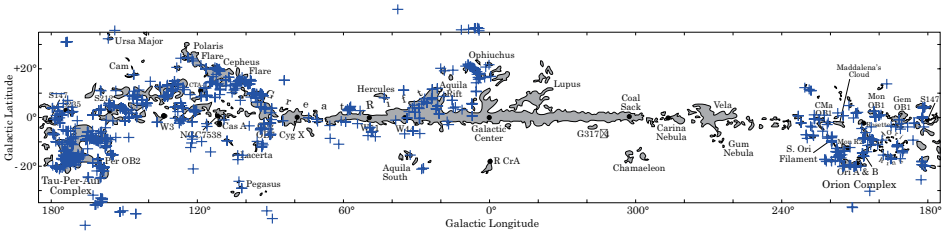

Figure 1: The *Planck* Cold Clumps studied by Wu et al. (2012) are plotted as +, over Milky Way regions map by Dame et al. (2001).

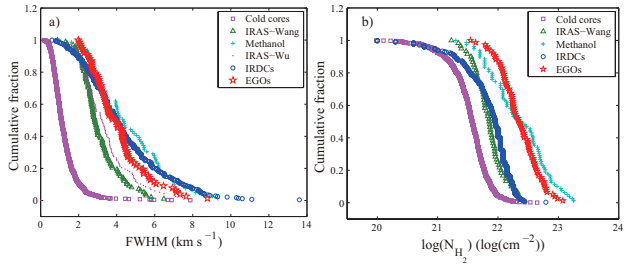

Figure 2: We compare the line widths of ^{13}CO(1-0) and column densities with the CO molecular line surveys toward different kind of targets.

On the top panel there is the spatial distribution of the sources of the single point observation, denoted as the blue crosses, overlayed on the Dame et al survey of the Milky Way. We observed all the Planck Cores that available to the PMO telescope, so we can see that most of the Planck Cores locate in several famous star forming regions: Orion, Taurus-Auriga, Perseus and California Complexes.

On the lower panel there is the statistics of the line width and column density derived from our observation. We made comparison with some other CO line surveys towards different kinds of targets, and our sources are as the purple dots here. We can see that our sources are with smallest line widths as well as lowest column density. Which is consistent with the expectation about Planck Cold Clumps: They should be quiet and primitive.

- Besides our single point study, we have conducted the mapping survey of the 71 Planck Cold Cores in Taurus Molecular Cloud (TMC), Perseus Molecular Cloud (PMC) and California Molecular Cloud (CMC).
- TMC contains ideal samples for studying characteristics of low mass star formation. Outflows (Wu et al. 2004), T Tau binary system (van Langevelde et al. 1994) , disks around HL Tau young stars (Sargent and Beckwith 1991), DM Tau (Saito et al. 1995) were all found in it. TMC contains class 0-III sources.
- PMC: intermediate mass star forming region (Lombardi et al. 2010). Star formation in PMC is between the low-mass (in TMC) and high-mass (in Orion) star formation (Johnstone et al. 2010).
- CMC is rarely studied before Lada et al. (2009). CMC is revealed similar to Orion in distance, mass and morphology, but with much lower star forming activity (Lada et al. 2009,Lombardi et al. 2010). In 2013, there is also a census of the YSO and the dense gas in CMC, using Herschel and CSO Harvey et al. (2013).

To understand Planck Cold Clumps in detail, especially the spatial distribution of its physical parameters, we need the mapping study besides our single point survey. I undertook the mapping study of seventy-one Planck Cold Clumps in the Molecular Clouds of Taurus, Perseus and California, which will be named as TMC, PMC and CMC hereafter.

TMC is a well known low mass star forming region. It is very near to us and the distance is only one-hundred-and-forty pc. Also, it contains many phenomena of star formation, like these ones. It contains sources of Class zero to three. All these facts prove that TMC is an ideal sample for studying star formation.

PMC is an set of intermediate mass star formation, which is between the high mass star formation in Orion and the low mass star formation of Taurus.

CMC is rarely studied compared to the two region above. It has not arose enough attention until the study of Lada et al in two thousand and nine. It has been revealed by the same research that having similar distance, mass and morphology as Orion, but with much lower star forming activity, which will be shown later also by our research.

Besides, there is a new-published survey of YSO and dense gas in CMC, using Herschel and CSO.

TMC: 34 sources; PMC: 13 sources; CMC: 24 sources.

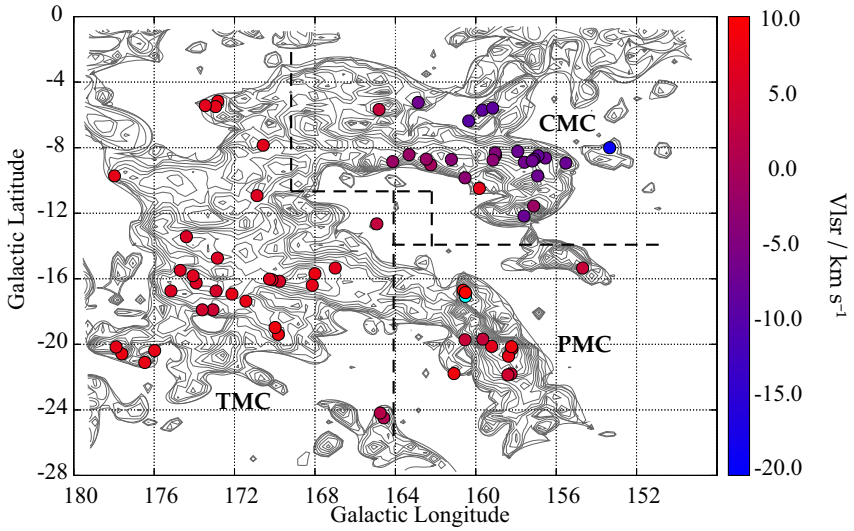

Figure 3: The 71 sources we mapped. Contours: CO integrated intensity map by Dame et al. (2001).

Here are how many sources are in the three regions respectively. Lower is the spatial distribution of the seventy-one mapped source, the colors represent the centroid velocity of the thirteen CO lines at there mapping center, overlayed also on the CO map by Dame et al.

2 Observation

The $J = 1 \rightarrow 0$ ^{12}CO , ^{13}CO and C^{18}O lines were observed using 13.7 m telescope of Qinghai Station of Purple Mountain Observatory, from January to May, 2011.

Condition of Observation

Half-power beam size	$56'' \times 55''$(at 92.8GHz)
Main beam efficiency	$\sim$50%
Pointing accuracy	better than $4''$
Spectral resolution	for ^{12}CO(1-0) : 0.16 km s^{-1}
	for ^{13}CO(1-0) , C^{18}O(1-0) : 0.17 km s^{-1}
T_A^* rms noise	for ^{12}CO(1-0) : 0.2 K
	for ^{13}CO(1-0) , C^{18}O(1-0) : 0.1 K
OTF scan speed	$20''$s^{-1}

This is the details of our observation, the spatial resolution is about one arc-minute times one arc-minute. And the spectral resolution, TA-star rms etc are as this.

Figure 4: Picture of PMO 13.7 m Telescope, from CAS website.

This is a picture of the telescope we used, on a altitude of three kilometers.

3 Results and Analysis

3.1 Gas Emission

- ^{12}CO(1-0) and ^{13}CO(1-0) emissions detected: all the 71 clumps
- C^{18}O(1-0) emissions detected: 55 clumps

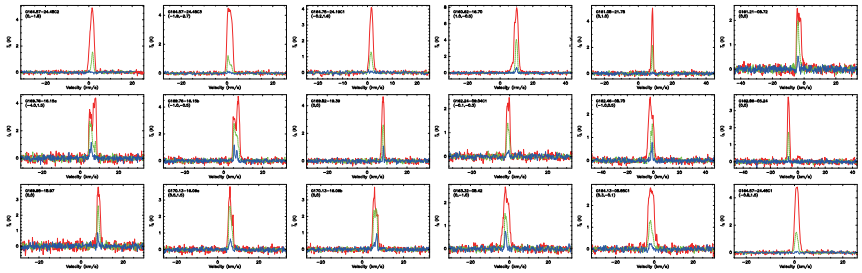

Figure 5: Examples of ^{12}CO(1-0) (red), ^{13}CO(1-0) (green) and C^{18}O(1-0) (blue) spectra detected at intensity peaks.

Here are some examples of the spectra we obtained. Lines of the three isotopes are in different colors.

Gaussian fitting was adopted for all three lines, and observed line parameters were obtained for each spectra.

Table 1: Observed line parameters (16 rows of the totally 82 rows)

Source	v_{lsr}(12) (km/s)	FWHM (12) (km/s)	Ta (12) (K)	v_{lsr}(13) (km/s)	FWHM(13) (km/s)	Ta(13) (K)	v_{lsr} (18) (km/s)	FWHM (18) (km/s)	Ta (18) (K)	
G154.68-15.34C1	3.37(0.07)	1.61(0.19)	4.09(0.74)	3.34(0.01)	0.96(0.03)	2.59(0.1)				
G156.92-09.72C1	-7.36(0.02)	2.23(0.05)	2.54(0.15)	-7.24(0.01)	1.39(0.03)	1.54(0.05)	-7.36(0.07)	1.12(0.28)	0.29(0.06)	BA
G157.12-11.56C1	-1.98(0.02)	1.96(0.04)	4.44(0.21)	-1.68(0.01)	1.23(0.02)	2.43(0.07)	-1.63(0.03)	0.87(0.06)	0.55(0.07)	
G157.12-11.56C2	-1.94(0.02)	2.05(0.05)	4.3(0.23)	-1.7(0.01)	1.28(0.03)	2.03(0.07)	-1.66(0.06)	0.88(0.12)	0.36(0.08)	
G157.12-11.56C3	-1.79(0.02)	2.19(0.06)	4.58(0.26)	-1.72(0.02)	1.14(0.05)	1.93(0.13)				W
G157.60-12.17bC1	-2.89(0.01)	2.53(0.02)	5.44(0.09)	-2.57(0.01)	1.15(0.03)	2.68(0.59)	-2.4(0.07)	0.71(0.14)	0.24(0.07)	
G157.60-12.17bC2	-2.44(0.02)	2.89(0.04)	5.11(0.18)	-1.97(0.03)	1.82(0.09)	1.69(0.11)				
G157.91-08.23C1	-7.28(0.02)	3.25(0.05)	2.38(0.11)	-7.31(0.01)	2.05(0.03)	1.92(0.07)	-7.49(0.05)	1.4(0.1)	0.53(0.08)	
G159.21-20.12C1	6.41(0.01)	4.44(0.01)	5.75(0.07)	6.63(0.01)	2.14(0.01)	4.88(0.06)	6.69(0.01)	1.2(0.03)	1.87(0.06)	
G160.51-17.07	10.41 (0.01)	2.82 (0.03)	5.92 (0.14)	10.43 (0.01)	1.57 (0.02)	3.46 (0.09)	10.6 (0.06)	1.13 (0.13)	0.49 (0.09)	
G160.53-09.84	-3.29 (0.01)	2.01 (0.01)	5.56 (0.09)	-3.51 (0.01)	1.44 (0.01)	2.88 (0.06)	-3.66 (0.03)	0.88 (0.09)	0.53 (0.07)	
G160.62-16.70	9.9 (0.01)	2.7 (0.02)	7.93 (0.17)	9.98 (0.01)	1.41 (0.01)	4.24 (0.07)	10.01 (0.04)	1.1 (0.08)	0.63 (0.07)	
G161.21-08.72	-3.27 (0.02)	3.04 (0.05)	2.42 (0.11)	-3.87 (0.02)	1.56 (0.04)	2 (0.09)	-3.78 (0.05)	0.91 (0.1)	0.51 (0.09)	
G163.32-08.42	-1.64 (0.02)	3.3 (0.04)	2.51 (0.09)	-1.78 (0.02)	1.64 (0.04)	1.48 (0.08)	-1.94 (0.03)	0.91 (0.06)	0.77 (0.08)	
G168.00-15.69	7.82 (0.03)	1.67 (0.07)	4.86 (0.37)	7.71 (0)	0.97 (0.01)	3.56 (0.06)	7.67 (0.01)	0.57 (0.02)	1.29 (0.07)	
G168.13-16.39	6.07 (0.03)	1.18 (0.06)	3.91 (0.14)	6.99 (0.02)	0.84 (0.05)	2.79 (0.08)	6.37 (0.02)	0.42 (0.06)	1.27 (0.1)	

• • •

We adopted Gaussian fitting for each of our spectrum and acquired the observed parameters, we posted some of these parameters at the emission peaks, including the centroid velocity, line width and antenna temperature of each isotope.

3.2 Physical Parameters

From the Gaussian fitting results, physical parameters such as excitation temperature (T_{ex}), column density of H_2 (N_{H_2}), velocity dispersions (σ_{Therm}, σ_{NT} and σ_{3D}) for each core and clump were derived.

$$T_{ex} = T_0 / \ln[T_0 (T_R^* + T_0 \exp(-T_0/T_{bg}) - 1)]$$

$$N_{tot} = \frac{3k}{8\pi^3 B \mu^2} \frac{\exp[hBJ(J+1)/kT_{ex}]}{(J+1)} \frac{(T_{ex} + hb/3k)}{[1 - \exp(-h\nu/kT_{ex})]} \int \tau_v \, dv \text{ (Garden et al. 1991)}$$

$$\sigma_{Therm} = \left(\frac{kT_{ex}}{m_H \mu} \right)^{1/2}, \sigma_{NT} = \left(\sigma^2_{^{13}\mathrm{CO}} - \frac{kT_{ex}}{m_{^{13}\mathrm{CO}}} \right)^{1/2} \text{ and } \sigma_{3D} = \sqrt{3(\sigma^2_{Therm} + \sigma^2_{NT})}$$

For them who have $C^{18}O$(1-0) detections.

$$\sigma_{NT} = \left(\sigma^2_{\mathrm{C^{18}O}} - \frac{kT_{ex}}{m_{\mathrm{C^{18}O}}} \right)^{1/2}$$

Employing the same methods, we calculated these parameters for every pixels ($0.5' \times 0.5'$) of each map.

From the observed parameters, and under the LTE assumption, we can derive the physical parameters such as excitation temperature, column density and velocity dispersion. The methods are as the following equations. To know the condition of turbulence in our samples, we separated the velocity dispersion into two parts, one is caused by thermal motion of molecules while one is caused by non-thermal motion such as turbulence. Notably, for the sources with C18O detection, we adopt the line width of C18O instead that of 13CO to avoid the optical depth effect.

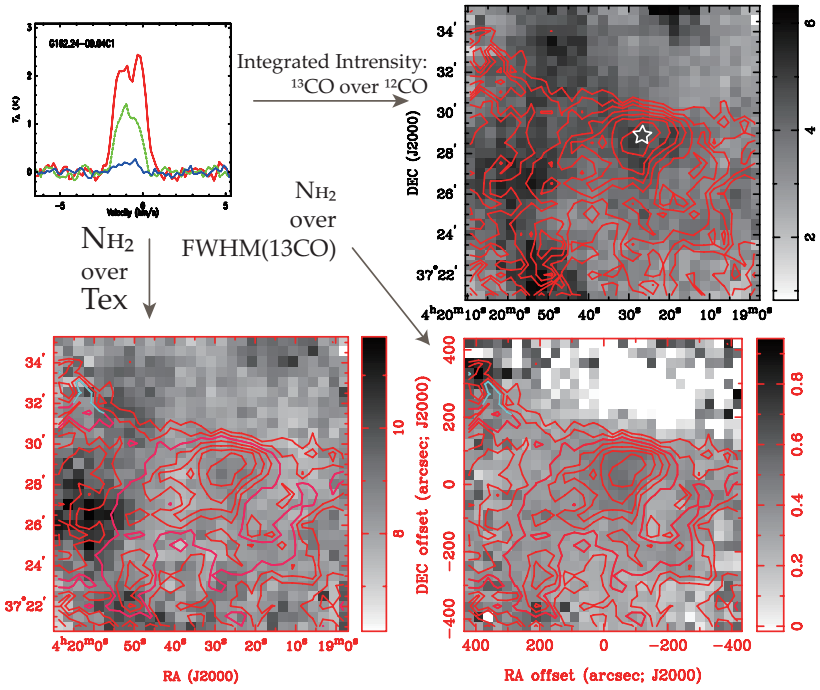

Instead of just focusing on the center of observation, we calculated these physical parameters of all the pixels of our mapping area, and got these parameters of every point. Like showed here.

From all the 71 clumps, we got the integrated intensity map for both ^{12}CO(1-0) and ^{13}CO(1-0) , Shown as red contours (^{12}CO) over greyscale background (^{13}CO).

We identified "cores" in our mapping areas, there are:

19 cores in TMC

16 cores in CMC

3 cores in PMC

Right shows one page of all the 5 pages of maps.

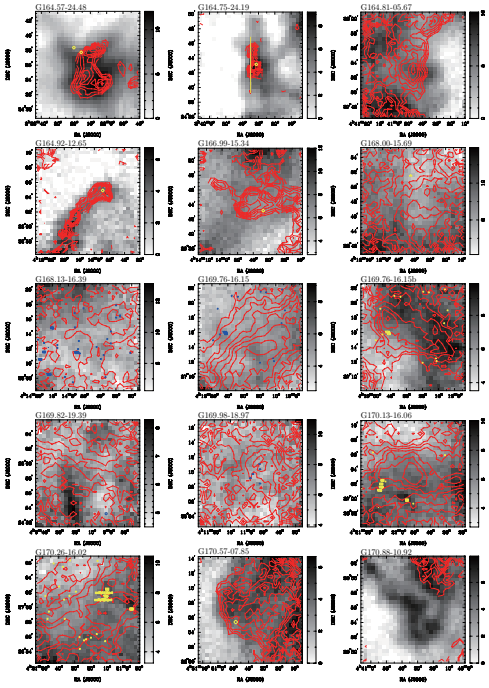

Here is one page of the totaly 5 pages of the integrated intensity maps, we identified some structures in our maps which show clear boundary and more definite sizes (such as this, this and this). We name them cores, to avoid the terminology of clumps used by Planck Collaboration and us to name the whole mapping area of fourteen time fourteen arc minute.

There are 19 cores in TMC, 16 in CMC while only 19 cores in PMC. We may exclude PMC in later statistical analysis because of the small number of cores in it.

Then we adopted the elliptic Gaussian fitting for these 13CO half maximum isolines of the cores and got their sizes.

Average value of physical parameters over mapping area within 50% peak intensity isolines for 38 cores were calculated.

Table 2: Physical parameters of cores(20 of 38 rows)

Name	V_{lsr}	Offset	Deconvolved Size	R	T_{ex}	N_{H_2}	σ_{Therm}	σ_{NT}	σ_{3D}	n	M_{LTE}	M_{vir}	M_J	Region
	$km\,s^{-1}$	($''$,$''$)	($'' \times ''(^\circ)$)	(pc)	(K)	(10^{21} cm^{-2})	($km\,s^{-1}$)	($km\,s^{-1}$)	($km\,s^{-1}$)	($\frac{10^3}{cm^{-3}}$)	($M_\odot$)	($M_\odot$)	($M_\odot$)	
G153.34-08.00C1	-18.93	(6 , -49)	196 × 107 (-13.2)	0.158	9.7 (0.5)	2.0 (0.7)	0.19(0.005)	0.34(0.04)	0.66(0.07)	2.0	2.9	43	19	CMC
G153.34-08.00C2	-19.10	(-163, 120)	224 × 86 (-21.0)	0.151	10.3(0.4)	1.5 (0.4)	0.19(0.003)	0.30(0.05)	0.60(0.07)	1.6	2.0	35	17	CMC
G154.68-15.34C1	3.31	(216 ,31)	1261× 381 (72.4)	0.394	11.9(0.9)	2.2 (0.7)	0.21(0.008)	0.32(0.09)	0.65(0.14)	0.9	20	76	28	PMC
G155.52-08.93C1	-7.46	(18 ,-2)	392 × 284 (-13.8)	0.364	9.7 (1.0)	1.0 (0.3)	0.18(0.009)	0.22(0.05)	0.48(0.07)	0.5	7.8	49	15	CMC
G156.92-09.72C1	-7.19	(50 , 53)	714 × 421 (-12.7)	0.598	9.0 (0.4)	1.8 (0.4)	0.18(0.004)	0.33(0.08)	0.64(0.13)	0.5	38	160	35	CMC
G157.12-11.56C1	-1.79	(-12 , 84)	383 × 238 (-55.4)	0.331	6.3 (0.9)	3.0 (0.7)	0.15(0.010)	0.26(0.05)	0.51(0.08)	1.5	19	53	10	CMC
G157.12-11.56C2	-1.90	(-50 , 137)	694 × 269 (-4.7)	0.473	6.2 (0.7)	2.7 (0.9)	0.15(0.009)	0.26(0.06)	0.52(0.09)	0.9	35	77	13	CMC
G157.12-11.56C3	-1.62	(-38 , -352)	173 × 102 (75.9)	0.145	5.3 (0.2)	2.4 (0.8)	0.14(0.003)	0.45(0.08)	0.81(0.13)	2.8	3.0	40	30	CMC
G157.60-12.17C1	-7.68	(67 , -45)	405 × 335 (-23.6)	0.402	10.5(1.0)	2.4 (0.8)	0.19(0.009)	0.28(0.09)	0.59(0.13)	0.9	23	76	20	CMC
G157.60-12.17bC1	-2.55	(-92 , -59)	513 × 372 (39.7)	0.476	14.9(1.5)	3.0 (0.9)	0.23(0.012)	0.21(0.10)	0.54(0.15)	1.0	40	50	14	CMC
G157.60-12.17bC2	-2.32	(-187, -266)	281 × 213 (61.4)	0.267	14.7(1.3)	2.9 (0.9)	0.23(0.010)	0.61(0.14)	1.11(0.23)	1.8	12	190	98	CMC
G157.91-08.23C1	-7.23	(31 , -106)	524 × 494 (31.6)	0.556	8.5 (0.6)	2.8 (0.8)	0.17(0.005)	0.41(0.13)	0.77(0.21)	0.8	51	230	47	CMC
G159.21-20.12C1	6.53	(47 , 3)	877 × 633 (-32.5)	0.425	16.1(1.3)	10.7(2.6)	0.24(0.010)	0.35(0.13)	0.74(0.21)	4.1	110	130	18	PMC
G159.67-05.71C1	-8.50	(-17 , -12)	469 × 418 (-9.4)	0.482	9.4 (0.6)	2.0 (0.9)	0.18(0.006)	0.51(0.13)	0.94(0.20)	0.7	27	410	90	CMC
G159.82-10.48C1	7.00	(23 , -7)	453 × 263 (-24.1)	0.376	12.4(0.7)	2.1 (0.7)	0.21(0.006)	0.41(0.09)	0.79(0.14)	0.9	17	150	49	CMC
G160.35-06.37C1	-9.2	(8 , -47)	238 × 79 (43.3)	0.149	8.6 (0.7)	1.3 (0.5)	0.17(0.008)	0.27(0.08)	0.55(0.11)	1.6	1.7	33	12	CMC
G160.53-19.72C1	3.56	(6 , 89)	864 × 473 (-62.6)	0.364	12.8(0.7)	4.2 (1.3)	0.21(0.005)	0.34(0.11)	0.71(0.18)	1.8	33	100	23	PMC
G162.24-09.04C1	-0.82	(-5 , -19)	562 × 377 (-78.6)	0.501	8.3 (0.4)	1.6 (0.5)	0.17(0.004)	0.37(0.08)	0.70(0.13)	0.5	23	230	45	CMC
G164.13-08.85C1	-1.66	(19 , -6)	709 × 372 (35.2)	0.559	9.9 (0.8)	2.3 (0.7)	0.19(0.008)	0.41(0.11)	0.78(0.17)	0.7	42	230	52	CMC
G164.57-24.48C1	0.90	(-49 , 90)	226 × 90 (-59.5)	0.048	12.6(0.6)	1.7 (0.5)	0.22(0.005)	0.35(0.07)	0.69(0.11)	5.6	0.23	19	14	TMC

• • •

Average value of physical parameters over mapping area within 50% peak intensity isolines for 38 cores were calculated. Presented here is one page as an example. We will only focus on cores instead of the clumps, because the former one are completely mapped.

3.3 Turbulence dominated cores

Most of the cores (in both TMC and CMC) are found with $\sigma_{NT} > \sigma_{Therm}$, indicating the dominance of turbulence.

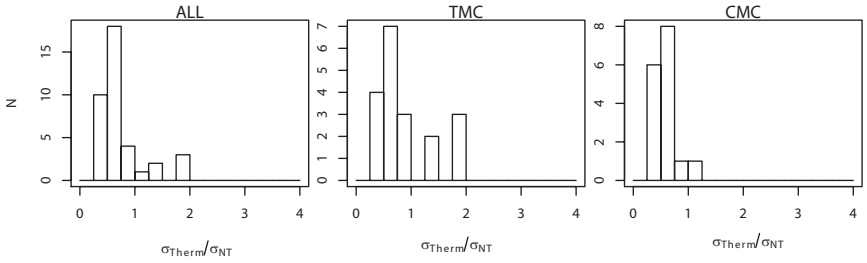

The dominance of turbulence indicates that the gravitational contracting/collapse is rare in our cores of both regions, otherwise the turbulence will soon decay on a dynamic timescale (Shu et al. 1987).

Firstly we compare the two parts of velocity dispersion, we found that most of our cores in both of TMC and CMC are with thermal-velocity-dispersion smaller than non-thermal ones. This plot shows the ratio of them two and we can see they are generally smaller than 1. After excluding the possibility of high-velocity gas by checking the line profile and P-V diagram we can see that the non-thermal motions are mainly caused by turbulence. Thus, this comparison actually indicates the dominance of turbulence. This dominance of turbulence is a suggestion that our cores do not have much contracting or collapse due to gravity, otherwise the turbulence will soon decay on a dynamical timescale, indicated by Frank Shu et al.

3.4 Stability of Cores

Most of the cores are found with LTE mass less than Jeans Mass and virial mass, indicating that these cores are generally stable.

TMC:

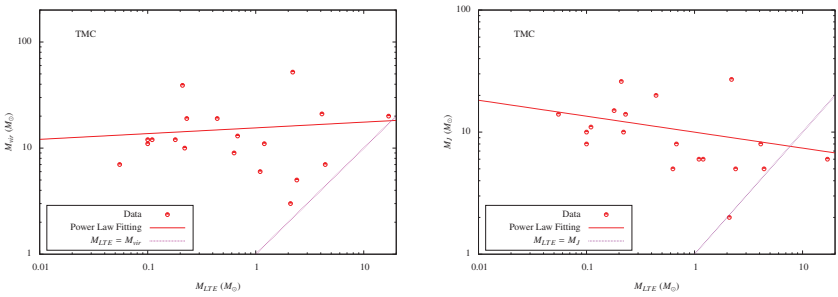

Left panel: The correlation between M_{LTE} and M_{vir}. Right panel: The correlation between M_{LTE} and M_J. The red line is the power law fitting function, while the blue dotted line is the $M_{LTE} = M_{vir}$line.

As we have already known the sizes and distance of our cores, we can calculate the LTE mass, Jeans mass and virial mass of them. By comparing this three masses, we can tell the stability of our cores.

We can see that in TMC, all the cores are with LTE mass smaller than the virial mass, and most of cores are with LTE mass smaller than Jeans mass, which indicates that the cores there are generally stable.

CMC:

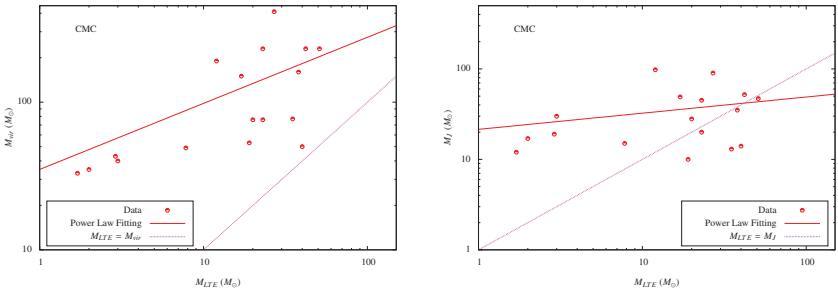

Left panel: The correlation between M_{LTE} and M_{vir}. Right panel: The correlation between M_{LTE} and M_J. The red line is the power law fitting function, while the blue dotted line is the $M_{LTE} = M_{vir}$line.

Situation in CMC is similar. However, we can note that six cores here are with Jeans mass exceeding their LTE mass. Which led to possibilities of collapsing, also for three of these six cores, thermal velocity dispersion are found larger than non-thermal velocity dispersion, which is consist with the possibility of collapsing.

4 Coupling of Gas and Dust

4.1 Temperature

Majority of the cores are found with $T_D > T_K$, consisting with the Goldreich-Kwan picture (Goldreich and Kwan, 1974).

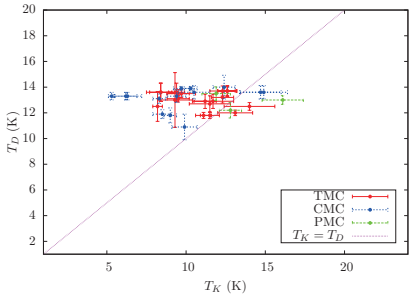

Figure 6: Correlation of Gas-Dust temperature

We compared the excitation temperature of our cores obtained from gas components against the temperature obtained from dust continuum emission. TK is kinetic temperature represent the temperature of gas while TD stands for dust temperature. We can see that for both TMC and CMC most of the cores are with dust temperature higher than their gas temperature. This consists well with the theory of Goldreich and Kwan, that dust heated by radiations firstly and then transfer the heat to gas by collisions between grains and molecules.

4.2 Column Density

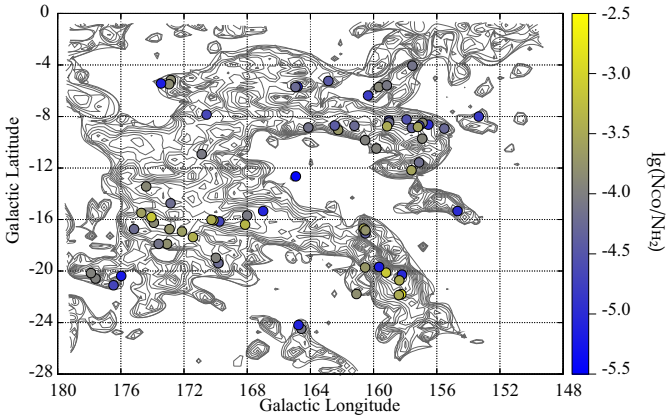

Figure 7: CO abundance calculated from CO emission ($N_{^{12}CO}$) and Planck ECC data (N_{H_2}); Background: The contours of ^{13}CO data from (Dame et al., 2001)

We have calculated the column density of CO. And we can also calculate the column density of H2 from Planck data of dust continuum emission. Thus we can calculate the ratio of these two column densities as the abundance of CO, and plotted this CO abundance map of our mapped regions. We can see that the center parts of each cloud are always with higher CO abundance.

5 Associated Objects

Most of the cores are without associated objects in the confine of circle of radius as same as beam size ($\sim$ 1 arc min) at there centers. The few exceptions are the cores that are:

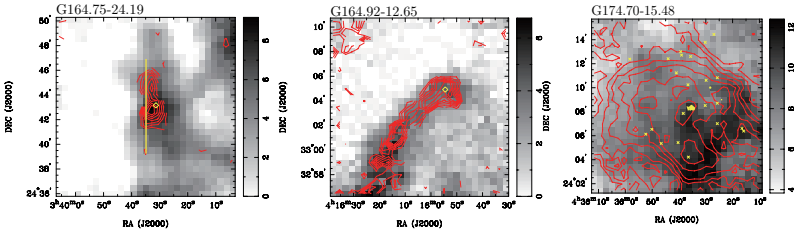

34 of 38 cores are without associated objects within their center parts, suggesting that they are sourceless. Remarkably, for the three cores with associated sources in TMC: G164.75-24.19C2 and G164.92-12.65C1 are both with σ_{Therm} larger than σ_{NT} . G174.70-15.48C1 is with $T_{ex}$of 14.0 K, which is the highest among the cores in TMC, also indication a later revolutionary stage.

We also checked the associated sources near the center of our cores, I mean within an offset of 1 arc-minute, as the same as the beam size. We can see that ninety percent of the cores are source-less and the three exceptions in TMC are as shown here.

These two are all with thermal velocity dispersion larger than non-thermal ones and this one is of temperature as high as fourteen Kelvin, highest among all the cores in TMC. All the three exhibit some hints of later evolutionary stage or star formation inside.

Despite this, from our study so far, most of our cores are still source less and not forming stars inside.

6 Summary

71 Planck cold clumps in TMC, CMC and PMC were mapped with ^{12}CO(1-0) , ^{13}CO(1-0) and C^{18}O(1-0) , respectively. Physical parameters such as T_{ex}, N_{H_2} , σ_{Therm} , σ_{NT} , σ_{3D} were calculated for the cores within them. By analyzing these physical parameters, several significant questions could be responded:

- What role turbulence plays in Planck cold clumps?
  - Turbulence dominates the cores, revealing Planck cores are generally immature.
- Are these clumps stable or have cores inside that will gravitationally collapse?
  - Majority of the cores are revealed stable in our research. But further study with higher resolution is still needed to warrant or deny it.
- How the gas and dust coupled?
  - Gas are slightly colder than dust for cores. CO abundance is higher in the center of complexes

---

From our observation, calculation and statistics of these Planck Cold Clumps, we can then answer these questions:

We can see turbulence are dominating the cores, indicating the lack of contracting or collapsing.

We can see that majority of our cores are stable, however, further study with higher spatial resolution are still needed to avoid that we have convolved several small cores into a big one.

Also, we can find that gas are sightly colder than dust, CO abundances are higher in the centers of three complexes.

- Are these cores sourceless or not?
  - Most of the cores are sourceless. For the cores associated with source, they show hints of collapsing.

These results suggest that Planck Cold Clumps are fairly excellent examples for studying the early stages of star formation and even the formation of molecular clouds.

The paper has been submitted to *ApJS* and has passed second review by the referee.

Also we prove that most of the cores are sourceless. For the cores associated with source, they show hints of collapsing.

All these facts above revealed by us prove that Planck Cold Clumps are ideal samples for studying the early stages of star formation and even the formation of molecular clouds from atomic clouds.

The paper about this research has been submitted to ApJS and has passed the second review.

Thanks!

Thanks!

References

Dame, T. M., Hartmann, D., and Thaddeus, P.: 2001, *ApJ* **547**, 792

Goldreich, P. and Kwan, J.: 1974, *ApJ* **189**, 441

Harvey, P. M., Fallscheer, C., Ginsburg, A., Terebey, S., André, P., Bourke, T. L., Di Francesco, J., Könyves, V., Matthews, B. C., and Peterson, D. E.: 2013, *ApJ* **764**, 133

Johnstone, D., Rosolowsky, E., Tafalla, M., and Kirk, H.: 2010, *ApJ* **711**, 655

Lada, C. J., Lombardi, M., and Alves, J. F.: 2009, *ApJ* **703**, 52

Lombardi, M., Lada, C. J., and Alves, J.: 2010, *A&A* **512**, A67

Planck Collaboration: 2011, *A&A* **536**, A22

Saito, M., Kawabe, R., Ishiguro, M., Miyama, S. M., Hayashi, M., Handa, T., Kitamura, Y., and Omodaka, T.: 1995, *ApJ* **453**, 384

Sargent, A. I. and Beckwith, S. V. W.: 1991, *ApJL* **382**, L31

Shu, F., Adams, F., and Lizano, S.: 1987, *ARA&A* **25**, 23

van Langevelde, H. J., van Dishoeck, E. F., and Blake, G. A.: 1994, *ApJL* **425**, L45

Wu, Y., Liu, T., Meng, F., Li, D., Qin, S., and Ju, B.: 2012, *Arxiv preprint arXiv:1206.7027*

Wu, Y., Wei, Y., Zhao, M., Shi, Y., Yu, W., Qin, S., and Huang, M.: 2004, *A&A* **426**, 503

Here are the references